Conformation Analysis of Aspartame-Based Sweeteners by NMR Spectroscopy, Molecular Dynamics Simulations, and X-ray Diffraction Studies

Antonia De Capua,[b, c] Murray Goodman†,[b] Yusuke Amino,[d] Michele Saviano,*[a] and Ettore Benedetti*[a]

Dedicated to the memory of Murray Goodman.

We report here the synthesis and the conformation analysis by ^{1}H NMR spectroscopy and computer simulations of six potent sweet molecules, N-[3-(3-hydroxy-4-methoxyphenyl)-3-methylbutyl]-α-L-aspartyl-S-tert-butyl-L-cysteine 1-methylester (**1**; 70 000 times more potent than sucrose), N-[3-(3-hydroxy-4-methoxyphenyl)-3-methylbutyl]-α-L-aspartyl-β-cyclohexyl-L-alanine 1-methylester (**2**; 50 000 times more potent than sucrose), N-[3-(3-hydroxy-4-methoxyphenyl)-3-methylbutyl]-α-L-aspartyl-4-cyan-L-phenylalanine 1-methylester (**3**; 2 000 times more potent than sucrose), N-[3,3-dimethylbutyl]-α-L-aspartyl-(1R,2S,4S)-1-methyl-2-hydroxy-4-phenylhexylamide (**4**; 5500 times more potent than sucrose), N-[3-(3-hydroxy-4-methoxyphenyl)propyl]-α-L-aspartyl-(1R,2S,4S)-1-methyl-2-hydroxy-4-phenylhexylamide (**5**; 15 000 times more potent than sucrose), and N-[3-(3-hydroxy-4-methoxyphenyl)-3-methylbutyl]-α-L-aspartyl-(1R,2S,4S)-1-methyl-2-hydroxy-4-phenylhexylamide (**6**; 15 000 times more potent than sucrose). The "L-shaped" structure, which we believe to be responsible for sweet taste, is accessible to all six molecules in solution. This structure is characterized by a zwitterionic ring formed by the AH- and B-containing moieties located along the +y axis and by the hydrophobic group X pointing into the +x axis. Extended conformations with the AH- and B-containing moieties along the +y axis and the hydrophobic group X pointing into the −y axis were observed for all six sweeteners. For compound **5**, the crystal-state conformation was also determined by an X-ray diffraction study. The result indicates that compound **5** adopts an L-shaped structure even in the crystalline state. The extraordinary potency of the N-arylalkylated or N-alkylated compounds **1–6**, as compared with that of the unsubstituted aspartame-based sweet taste ligands, can be explained by the effect of a second hydrophobic binding domain in addition to interactions arising from the L-shaped structure. In our examination of the unexplored D zone of the Tinti–Nofre model, we discovered a sweet-potency-enhancing effect of arylalkyl substitution on dipeptide ligands, which reveals the importance of hydrophobic (aromatic)–hydrophobic (aromatic) interactions in maintaining high potency.

Introduction

In our efforts to determine the molecular basis and structural requirements for the sweet taste, it has been a goal of our laboratories to develop useful molecular models for taste recognition. Our approach toward this end integrates the study of taste profiles with the design, synthesis, and conformation analysis of novel ligands. In constructing predictive taste models, we have sought to determine the active conformations of sweet taste ligands.

Over the years, a number of methods have been applied to examine the conformation preferences of potent sweet taste ligands. Walters et al.[1] reported the use of computational methods to find conformational similarities within a set of high-potency sweeteners. The resulting topological agreements form a tentative model for sweet taste, although comparisons are made among peptide and nonpeptide structures. These findings raise the question as to whether all sweet compounds bind to the same receptor with similar conformational features.

[a] Dr. M. Saviano, Prof. E. Benedetti
Institute of Biostructures and Bioimaging, CNR
Department of Biological Sciences
University of Naples "Federico II" and C. I. R. Pe. B.
Via Mezzocannone 16, 80134 Naples (Italy)
Fax: (+39) 081-2534560
E-mail: msaviano@unina.it
ettore.benedetti@unina.it

[b] Dr. A. De Capua, Prof. M. Goodman
Department of Chemistry and Biochemistry
University of California, San Diego
La Jolla, CA 92093-0343 (USA)

[c] Dr. A. De Capua
Current address:
Second University of Naples, Department of Environmental Science
via Vivaldi 43, 81100 Caserta (Italy)

[d] Dr. Y. Amino
Ajinomoto Co., Inc., AminoScience Laboratories
1-1 Suzuki-Cho, Kawasaki-Ku, Kawasaki-Shi 21-8681 (Japan)

Recently, Morini et al.[2a] and Xu et al.[2b] have proposed that sweet proteins recognize a binding site different from the one that binds small-molecular-mass sweeteners. Therefore, we have restricted our studies to peptide-based Asp-like sweeteners. To obtain active ligand conformations for the investigation of these interactions, we utilize a combination of NMR spectroscopy, molecular modeling, and X-ray diffraction studies. We believe this combination of biophysical data provides the most effective way to arrive at the topochemical requirements for sweet taste.

The taste recognition model shown in Figure 1 describes the relationship between topochemical array and taste in aspartyl-based ligands.[3] The zwitterionic glucophore (termed AH/B) of
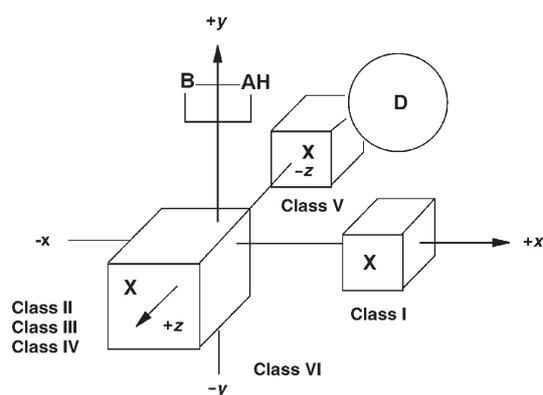
Figure 1. A schematic illustration of the relationship between topochemical arrays of the AH, B, X, and D glucophores and tastes of dipeptide-based ligands. Sweet: classes I, VI; bitter: class V; tasteless: classes II, III, IV; D zone: key to the enhancement of sweet potency.

group. The D zone is an interesting region because we believe it to be an essential spatial component that enhances the potency of sweet ligands. By placing the Tinti–Nofre model on the Cartesian coordinates and arraying an L-shape aspartame conformer, it is seen that the G region of the Tinti–Nofre model superposes on the X region of the class I conformer in Figure 1. The D zone remains unexplored in terms of molecular arrangement.[6] As a result, we sought to design and synthesize sweet ligands to probe this latter zone and to determine its role in sweet taste potency. In the previous paper, we analyzed some N-arylalkyl aspartame-based sweet ligands and proposed that the structures of the arylalkyl group in the D zone are the key to the major enhancement of the sweet potency (for example, compound **7** in Scheme 2).[6]

In the present study, we designed, synthesized, and analyzed the six N-substituted aspartame-based sweet ligands shown in Scheme 1. The original, unsubstituted aspartame-based sweet taste ligands **8**, **9**, and **11** in Scheme 2 are 900, 225, and 2500 times more potent than sucrose, respectively.[7–9] Ligand **10** is faintly sweet.[10] These four ligands contain the characteristic hydrophobic groups in the X region. However, the N-arylalkyl- or N-alkyl-substituted analogues of these ligands elicit an extremely strong sweet taste. The conformational features and the chemical structures of the X region and the D zone of these molecules were then correlated to their taste properties in an effort to probe the molecular basis of taste of aspartame-based sweeteners.

the Shallenberger–Kier[4] model is oriented on the +y axis, and the hydrophobic group plays a decisive role in determining the taste class of the ligand. From the stand point of the taste recognition model in Figure 1, of the two conformers that contribute to the sweet taste of the Asp-based ligands the "L-shaped" hydrophobic glucophore occupies the +x axis region of space (class I) and the extended glucophore lies along the −y axis (class VI).

The Tinti–Nofre model for sweet taste ligands[5] assigns spatial regions to a number of pharmacophoric groups considered to be essential for sweet taste. The G domain of this model can be viewed as equivalent to the X domain in the Shallenberger–Kier model since it accommodates the hydrophobic

Scheme 1. Sweet taste ligands with N-arylalkyl or N-alkyl substitution.

Results

X-ray diffraction analysis

Figure 2 shows a stereodrawing of a molecular model of compound **5**, as determined by X-ray diffraction analysis. Selected conformational angles found experimentally are given in
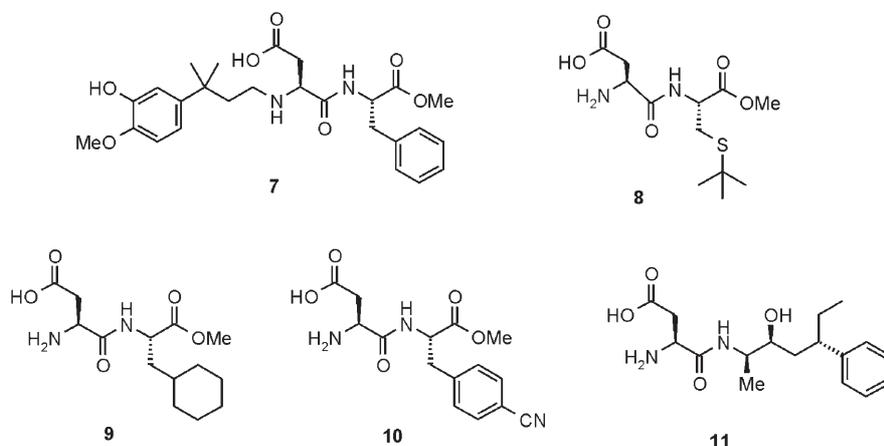
Scheme 2. Aspartame-based sweet taste ligands.
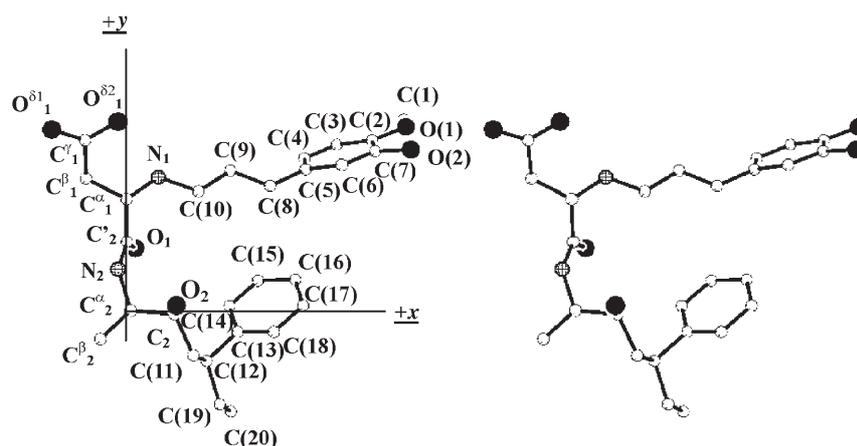
Figure 2. Stereodrawing of the molecular model of compound **5**, as obtained by X-ray diffraction analysis, with the atom numbering.

Table 1. The intermolecular H-bond parameters are reported in Table 2. As usually observed in dipeptides of the aspartame family, the substituted N-terminal Asp moiety exists as a zwitterion. The molecule has the L-aspartyl residue in the conformation usually observed in Asp-based dipeptide analogues.[3] This conformation shows dihedral angles ψ_1, ω_1, χ_1^1, and $\chi_1^{2,1}$ for the Asp residue of $+144°$, $-157°$, $-73°$, and $-148°$ (or $+33°$ for $\chi_1^{2,2}$), respectively. The torsion angle about the Asp C^α–C^β bond (χ_1^1) is gauche$^-$ (g^-). The carboxylate group of the Asp side chain is nearly coplanar with the C^α–C^β bond: the $\chi_1^{2,1}$ and $\chi_1^{2,2}$ dihedral angles are $-148.1°$ and $33.3°$, respectively. A significant deviation of the ω torsion angle from the ideal value angles of the *trans* planar peptide ($180°$) is observed: the peptide ω_1 value differs by $23°$.

The overall spatial arrangement of the AH, B, and X glucophores is mainly defined by the torsion angles of the residues after the L-Asp (Table 1), since the angles ψ_1, ω_1, χ_1^1, and $\chi_1^{2,1}$ do not substantially change the disposition of the AH and B groups relative to the backbone chain. The conformation observed corresponds to an L-shaped structure in which the AH- and B-containing zwitterionic ring of the Asp moiety forms the stem of the L shape along the $+y$ axis, and the hydrophobic X group, represented by the C-terminal phenyl ring, projects along the base of the L shape along the $+x$ axis (Figure 2).

The packing mode of the compound is mainly governed by two intermolecular H-bonds (N_1–H···O_2=C'_2 and $O(2)$–H···$O^{\delta 1}_1$=C^γ_1; Table 2), which give rise to rows of molecules H-bonded along the *b* and *c* directions, respectively. In addition, two other H-bonds stabilize the structure, by involving the Asp side chain (N_2–H···$O^{\delta 2}_1$=C^γ_1 and O_2–H···$O^{\delta 1}_1$=C^γ_1) of symmetry-related molecules by the 2_1 axis. Hydrophobic interactions further contribute to crystal packing.

NMR spectroscopy analysis and molecular dynamics simulation

The experimental data for all six compounds obtained from one- and two-dimensional ^{1}H NMR spectroscopy are given in the Supporting Information.

Molecular dynamics simulation covers all the conformational

Table 1. Relevant torsion angles [°] for *N*-[3-(3-hydroxy-4-methoxyphenyl)propyl]-α-L-aspartyl-(1*R*,2*S*,4*S*)-1-methyl-2-hydroxy-4-phenylhexylamide (**5**).		
Torsion angle		
C(9)-C(10)-N$_1$-C$^\alpha_1$	"ω_0"	−178.1(3)
C(10)-N$_1$-C$^\alpha_1$-C$'_1$	"ϕ_1"	−66.6(4)
N$_1$-C$^\alpha_1$-C$'_1$-N$_2$	ψ_1	144.0(3)
C$^\alpha_1$-C$'_1$-N$_2$-C$^\alpha_2$	ω_1	−157.0(3)
N$_1$-C$^\alpha_1$-C$^\beta_1$-C$^\gamma_1$	χ_1^1	−72.6(4)
C$^\alpha_1$-C$^\beta_1$-C$^\gamma_1$-O$^{\delta 1}_1$	$\chi_1^{2,1}$	−148.1(3)
C$^\alpha_1$-C$^\beta_1$-C$^\gamma_1$-O$^{\delta 2}_1$	$\chi_1^{2,2}$	33.3(5)
C$'_1$-N$_2$-C$^\alpha_2$-C$_2$	"ϕ_2"	84.6(4)
N$_2$-C$^\alpha_2$-C$_2$-C(11)	"ψ_2"	−176.2(3)
C$^\alpha_2$-C$_2$-C(11)-C(12)	"ω_2"	78.5(5)
C$_2$-C(11)-C(12)-C(19)		−173.3(4)
C(11)-C(12)-C(19)-C(20)		177.2(5)
C$_2$-C(11)-C(12)-C(13)		61.9(6)

Table 2. Intermolecular H-bond parameters for compound **5**.				
Donor	Acceptor	Length (N···O) [Å]	Angle (C'=O···N) [°]	Symmetry operation
N_1	O_2	2.723(5)	152.1(2)	$x, -1+y, z$
N_2	$O^{\delta 2}{}_1$	3.010(4)	107.4(2)	$-x, 1/2+y, 1-z$
O_2	$O^{\delta 1}{}_1$	2.717(4)	116.9(2)	$-x, 1/2+y, 1-z$
O(2)	$O^{\delta 1}{}_1$	2.669(4)	131.1(2)	$x, y, 1+z$

space available to the molecules. Since the molecules are very flexible in solution, the number of accessible conformations in this state is large. In this study, the low-energy structures derived from dynamics simulation were clustered according to the torsion angles of the backbone. The final results were categorized according to the arrangement of the glucophore groups.[3]

The strong NOE between the α-proton of Asp and the amide proton of the residue in position 2, as well as the $^3J_{HN-H\alpha}$ coupling constants, indicate that the peptide bond is in the *trans* conformation for all analogues. The side-chain populations for Asp and residue 2 are g^- for compounds **1–3**, a conclusion predominantly based on their $^3J_{H\alpha\beta}$ coupling constants and side-chain NOE values. The side-chain population for Asp in compound **4** could not be determined because of chemical-shift overlapping of β protons. The calculated rotamer populations for Asp in compounds **5** and **6** were predominantly determined as g^-.

The torsion angles of the mean minimum-energy structures from cluster analysis are included in Tables 3 and 4 for analogues **1–3** and **4–6**, respectively, and the corresponding typical structures are shown in Figures 3–8. These conformations are consistent with the NMR data.

The NMR data and dynamic simulations have suggested that all the compounds examined in this investigation can adopt L-shaped and extended conformations, while none of them has access to conformations with significant extension into the −z

axis, which is the structural array for the bitter taste.[11] All these compounds are in fact sweet analogues.

Compound 1: Analogue **1** exhibits a potency about 70 000 times that of sucrose. As far as the side-chain population of Asp is concerned, the g^- orientation seems to be the most populated conformation in solution. The side chain of residue 2, CH₂−S(CH₃)₃, shows preference for the g^- orientation, a result that is identical to those obtained for H−Asp¹−Phe²−OMe and related compounds. In H−Asp¹−Phe²−OMe and in various other Phe-containing sweet-tasting dipeptides, the Phe side chain prefers the g^- conformation. The torsion angles of the mean minimum-energy structures from cluster analysis for compound **1** are summarized in Table 3. The structures are shown in Figure 3. Conformations **a** and **c** represent the L-shaped structure. The hydrogen-donor AH and -acceptor B of the Asp residue form a zwitterion on the stem of the L shape along the +y axis, and the hydrophobic-group side chain of residue 2, CH₂−S(CH₃)₃, projects along the base of the +x axis. The N-terminal arylalkyl chain is parallel (that is, in the +x, +y quadrant) to the hydrophobic moiety X (that is, the side chain of residue 2, CH₂−S(CH₃)₃). Conformation **b** is an extended structure with the AH and B moieties along the +y-axis and the hydrophobic group X (CH₂−S(CH₃)₃) pointing to the −y direction.

Compound 2: Analogue **2** is 50 000 times more potent than sucrose. It shows L-shaped and extended conformations (Figure 4). In particular, conformations **b**–**d** represent L-shaped structures and differ in the orientation of the Asp side chain, which is g^+ in **b**, *trans* in **c**, and g^- in **d**. The result shows that the Asp side chain is not fixed but adopts all three rotamers. The hydrophobic group side chain of residue 2 in conformers **b**–**d** has a preference for the g^- conformation, even though overlapping of β-proton signals does not allow the calculation of the experimental conformation of all three rotamers separately. Structure **a** represents the extended conformation: the Asp side chain and the hydrophobic group of residue 2 are both in the *trans* conformation.

Table 3. Torsion angles [°] of the mean minimum-energy structures from cluster analysis for compounds **1–3**.[a]										
					Compound **1**					
	ϕ_1	ψ_1	ω_1	χ^1_1	ϕ_2	ψ_2	ω_2	χ^1_2	σ_1	σ_2	σ_3
a	−122	159	−178	−62	−106	119	−179	−60	−178	−176	174
b	−177	168	−179	177	−116	117	−179	−175	−179	177	175
c	−58	135	−177	−57	−78	120	−179	−63	−176	−174	−179
					Compound **2**					
	ϕ_1	ψ_1	ω_1	χ_1	ϕ_2	ψ_2	ω_2	χ^1_2	σ_1	σ_2	σ_3
a	−175	110	−179	143	−82	94	−179	−162	−50	140	179
b	−157	128	−179	73	−96	88	−179	−73	−179	−179	179
c	−121	129	−179	−132	−22	83	−179	−70	0	154	−179
d	−122	104	−179	−73	−121	87	−179	−69	177	176	179
					Compound **3**					
	ϕ_1	ψ_1	ω_1	χ_1	ϕ_2	ψ_2	ω_2	χ^1_2	σ_1	σ_2	σ_3
a	−172	63	−178	47	−129	86	−179	−59	−179	179	179
b	−173	160	−179	52	−126	85	−179	−73	179	−179	179
c	−172	63	−179	47	−136	−83	179	50	−179	179	179
d	−172	157	−179	51	−139	−84	179	−164	179	−178	179
e	−174	166	179	54	−176	102	−179	62	−179	178	179
[a] σ_1: C1-C2-C3-C4; σ_2: AspN-C1-C2-C3; σ_3: AspC$^\alpha$-AspN-C1-C2.											

Compound 3: In analogue **3** the Asp side chain shows a clear preference for the g^+ rotamer and the hydrophobic-group side chain of residue 2 (4-cyanophenyl) shows a preference for the g^- orientation. The torsion angles of the minimum-energy conformations of each cluster are summarized in Table 3. The structures are shown in Figure 5. Conformation **e** represents an L-shaped structure with the zwitterionic ring forming the stem of the L shape and the hydrophobic group of residue 2 (4-cyanophenyl) projecting along the $+x$ axis. The arylalkyl chain at the N terminus tends to be parallel to the $+y$ axis line. Conformations **a** and **c** are L-shaped structures as well, but the orientation of the 4-cyanophenyl ring points into the area between the $+y$ and $+z$ axes (out of the x–y plane). These structures have the hydrophobic-group side chain of residue 2 (4-cyanophenyl) pointing into the $+z$ dimension. Moreover, in the L-shaped structure **b**, the side chain of residue 2 (4-cyanophenyl) points into the area between the $+x$ and $+y$ axes. Conformation **d** is an extended structure with a considerable $-y$ component.

Compound 4: In compound **4** the Asp side chain shows a clear preference for the g^+ rotamer. The torsion angles of the minimum-energy conformations of each cluster, are summarized in Table 4 and the structures are shown in Figure 6; the angles define conformation families that are consistent with the experimental data. Structure **e** is an extended structure with the hydrophobic phenyl ring projecting along the y axis. Structures **a**–**c** are similar structures; however, the hydrophobic phenyl group is pointing into the $+z$ axis. Structure **f** is an L-shaped conformer with the hydrophobic group pointing along the $+x$-axis. The **d** structure is a conformation with a reversed L-shaped structure which has the hydrophobic phenyl moiety projecting along the $-x$ axis. As for the L-shaped conformer,
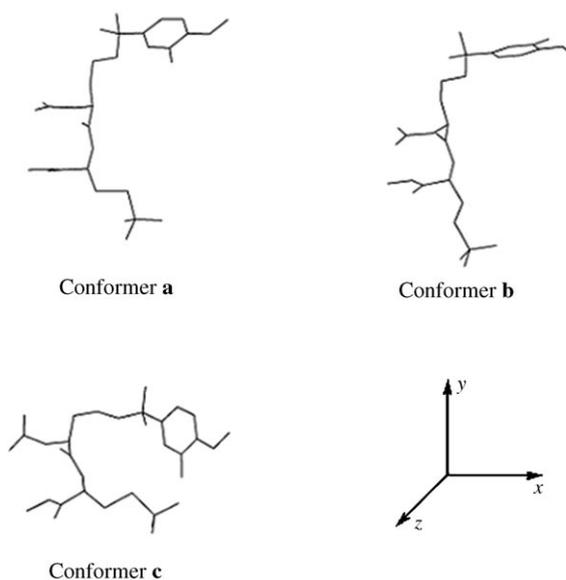
Figure 3. Mean structures from cluster analysis of compound **1**.
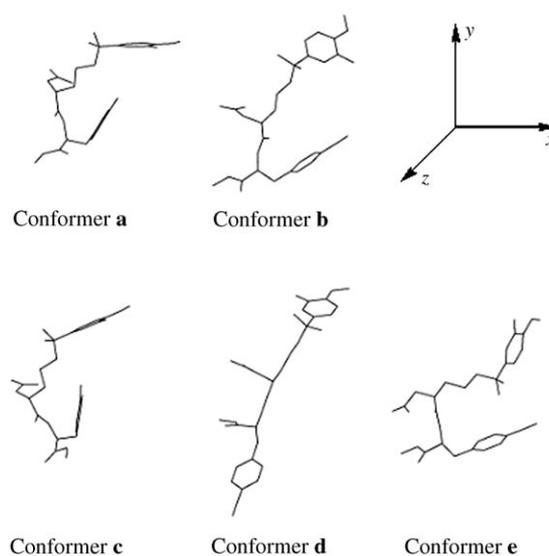
Figure 5. Mean structures from cluster analysis of compound **3**.
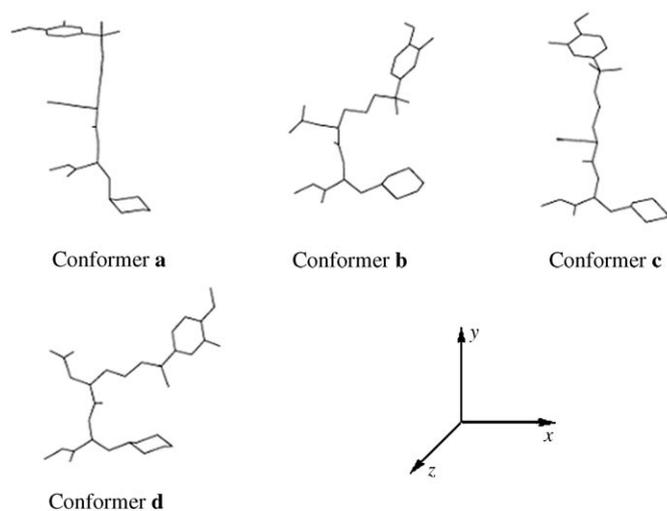
Figure 4. Mean structures from cluster analysis of compound **2**.
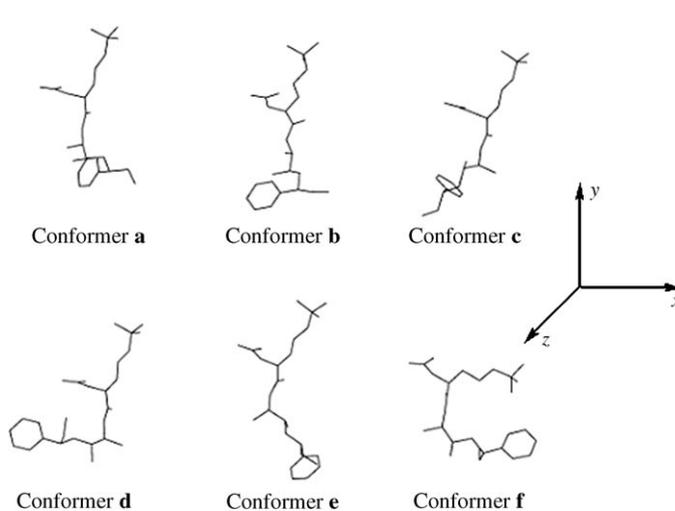
Figure 6. Mean structures from cluster analysis of compound **4**.

Table 4. Torsion angles of the mean minimum-energy structures from cluster analysis for compounds **4**–**6**.[a]

	ϕ_1	ψ_1	ω_1	χ_1	ϕ_2	ψ_2	ω_2	σ_1	σ_2	σ_3	σ_4	σ_5
					Compound 4							
a	−174	158	179	50	−62	−49	−179	−	−	−57	−55	
b	−174	165	−179	53	151	−61	−179	−	−	168	−174	
c	−174	165	−179	53	151	−61	−179	−	−	169	−65	
d	−173	165	179	53	−176	−160	179	−	−	−168	174	
e	−174	164	179	52	115	−164	179	−	−	−169	174	
f	−71	148	179	55	116	−59	−179	−	−	−63	−58	
					Compound 5							
a	−173	163	−179	52	117	−55	179	179	179	−179	−167	174
b	−171	55	−179	49	107	−54	179	−179	179	−179	−167	174
c	−64	−45	−179	54	123	−53	179	175	179	64	−168	174
d	−176	163	179	51	115	−165	179	178	179	−63	−61	177
					Compound 6							
a	−177	174	178	54	−74	−56	179	105	−179	−59	49	62
b	−174	60	179	49	−75	−162	179	179	179	−179	−61	177
c	−174	163	179	54	−76	−160	179	178	179	−179	−169	65
d	−68	139	179	−61	−61	−53	−68	−179	179	−179	−177	175

[a] σ_1: Asp N-C1-C2-C3; σ_2: AspC$^\alpha$-AspN-C1-C2; σ_3: C1-C2-C3-C4; σ_4: C$^\beta$-C$^\gamma$-C$^\delta$-C$^\varepsilon$; σ_5: C$^\gamma$-C$^\delta$-C$^\varepsilon$-C$^\eta$.

the N-terminal chain in the reversed structure is also parallel to the X group but the two groups project to opposite directions.

Compounds 5 and 6: The structures for compounds **5** and **6** are shown in Figures 7 and 8, respectively. For compound **5**, structure **a** is an L-shaped structure with the hydrophobic group pointing along the $+x$ axis and structure **d** is a reversed L-shaped conformation. Conformations **b** and **c** are extended structures with a considerable $-y$ component. For compound **6**, structure **d** is an L-shaped structure and structure **b** is a reversed L-shaped conformation. Conformations **a** and **c** are extended structures with a considerable $-y$ component.

Discussion

The six sweet-tasting Asp-based compounds can be divided in two groups based on their different chemical substitutions. The first group comprises compounds **1**–**3**; these compounds contain different hydrophobic groups X in the side chain of the second residue but the same N-terminal arylalkyl chain. The second group comprises analogues **4**–**6**, where only the N-terminal group is changed while residue 2 is substituted with the [2-(*S*)-hydroxy-1-(*R*)-methyl-4-(*S*)-phenyl-hexylamide] alkyl chain.

The NMR spectroscopy data and dynamics simulation indicate that all compounds examined in this paper can adopt the L-shaped, the reversed L-shaped, or the extended conforma-

Conformer **a**   Conformer **b**

Conformer **c**   Conformer **d**
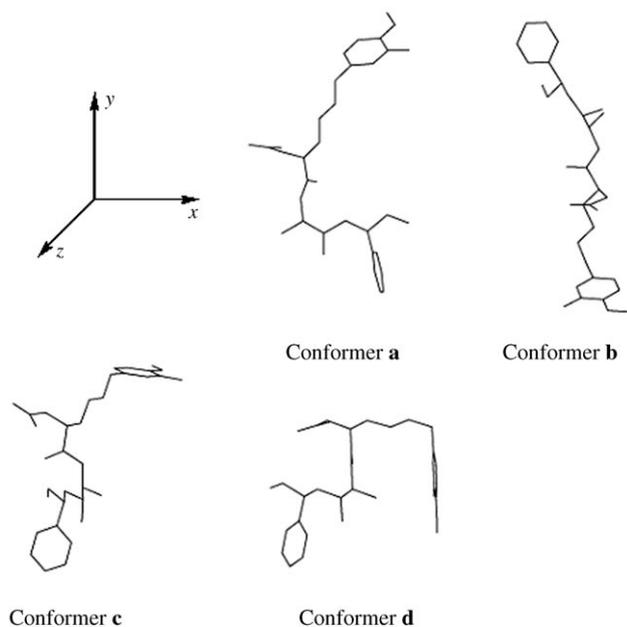
Figure 7. Mean structures from cluster analysis of compound **5**.

Conformer **a**   Conformer **b**

Conformer **c**   Conformer **d**
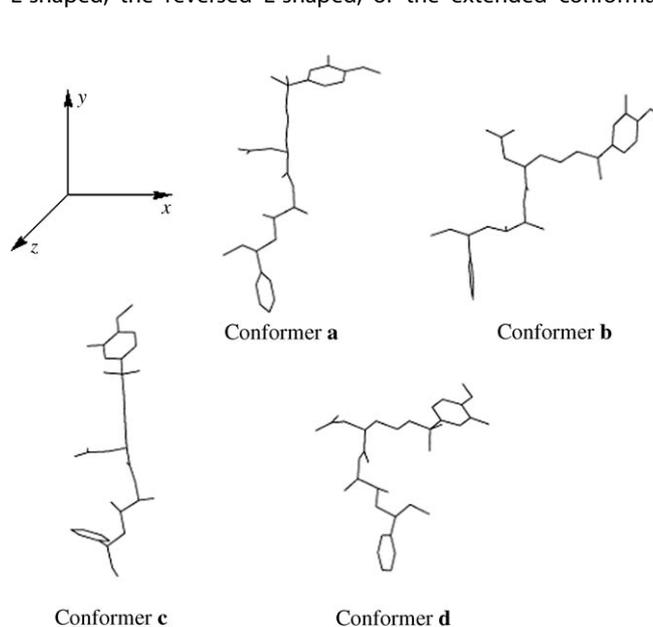
Figure 8. Mean structures from cluster analysis of compound **6**.

tions with a +z array of the hydrophobic side-chain moiety of residue 2 (X). None of the ligands exhibits conformations with significant extension into the −z axis; these conformations were proposed for bitter-taste peptide-based ligands.[3]

Compound **1** preferentially adopts L-shaped conformations. A further study of molecular dynamics was conducted to investigate the flexibility of the backbone and the relative orientation of the two hydrophobic groups (N-terminal arylalkyl chain and hydrophobic moiety X of residue 2). In Figure 9 the trajectories from the 1 ns unrestrained molecular dynamics simulations of analogue **1** at 300 K are shown.

It can be concluded that compound **1**, during the time period of the molecular dynamics simulation, tends to assume preferentially an L-shaped conformation where the arylalkyl and the hydrophobic group of residue 2 (CH_2–$S(CH_3)_3$) lie parallel to each other so that the N-terminal arylalkyl group is arrayed above the base of the L shape. The conformation of the N-terminal arylalkyl group and the hydrophobic group of residue 2 does not alter the zwitterionic nature of the molecule nor the L-shaped structure. Instead, the substitution of the CH_2–$S(CH_3)_3$ group strongly enhances the sweetness potency of this taste ligand. The presence of both a hydrophobic site above the base of the L shape and the specific hydrophobic group, CH_2–$S(CH_3)_3$, forming the base of the L shape could be responsible for the extraordinary sweetness potency of this compound.

For compound **2** the L-shaped structures are accessible as well. The substitution of a hydrophobic moiety of residue 2 also enhances the sweetness potency of this compound but probably also increases its flexibility.

Compound **3** can assume several conformations, namely, extended and different L-shaped conformations having both the hydrophobic group oriented into the +z axis and along the

+x-axis. It is interesting to note that in these conformations the hydrophobic, 4-cyanophenyl group of residue 2 and the N-terminal arylalkyl portion tend to be further apart, thus showing more flexibility in the relative orientation of the two hydrophobic groups. To investigate the flexibility of the backbone and the relative orientation of the two hydrophobic groups, as in compound **1**, a further study of unrestrained molecular dynamics at 1 ns and 300 K was carried out. The overlay of the extended and the +z conformations for analogue **3** is shown in Figure 10. The very large flexibility shown by compound **3** could be due to the presence of the bulky 4-cyanophenyl hydrophobic group of residue 2 which does not allow the formation of the regular L-shape conformation, probably because of a hydrophilic interaction between the 4-cyanophenyl group and the polar groups (NH_2^+ and the side-chain COO^- of Asp) forcing it to point towards the aromatic ring (Figure 10). To investigate this hypothesis more deeply, we compared the differences of the topochemical array with the pharmacophore model based on the Tinti–Nofre theory[5] for each analogue. We calculated the distances between the binding sites in the pharmacophore model proposed by Tinti–Nofre for analogues **1**–**6**. It is interesting to note that the distances between the binding sites G (side chain of residue 2) and D (N-terminal group), G and AH (polar group NH_2^+ of the Asp residue), and G and B (COO^- of the Asp side chain) in analogue **3** are 9.5, 5.4, and 6.6 Å, respectively. In the most potent analogues, **1** and **2**, the analogous distances are 10.3, 9.04, and 9.3 Å (analogue **1**) and 10.5, 7.2, and 8.8 Å (analogue **2**). It is evident that the less potent of the analogues (**3**) shows a smaller distances. After analyzing the structures from the molecular dynamics simulations (Figure 10), we believe that this decrease in the distances is probably due to a hydrophilic interaction between
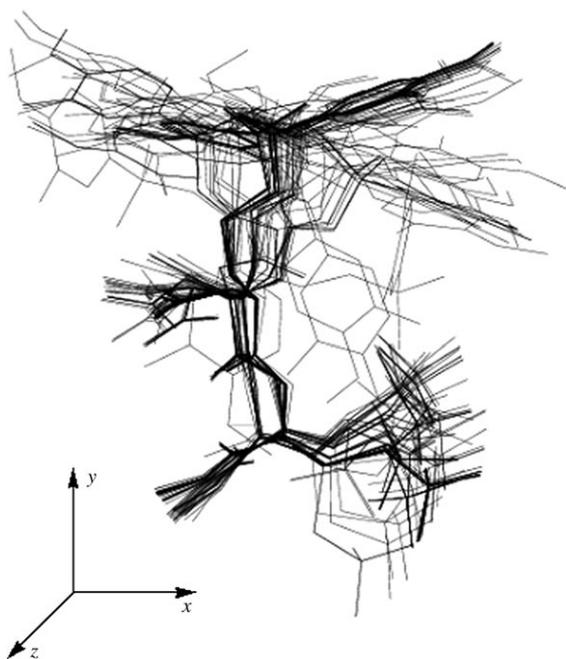
Figure 9. Trajectories from the 1 ns unrestrained molecular dynamics simulations of compound **1** at 300 K.

Figure 10. Trajectories from the 1 ns unrestrained molecular dynamics simulations of compound **3** at 300 K.

the 4-cyanophenyl hydrophobic group of residue 2 and the polar groups NH_2^+ and COO^- which does not allow the formation of the regular L shape. This behavior is not met in analogues **1** and **2**, where the distances are sufficiently long and do not affect the correct L-shaped topology.

As for compounds **4–6**, they can adopt multiple conformations in solutions, namely, extended, L-shaped, reversed L-shaped, and L-shaped pointing in the $+z$ dimension. We believe that the substitution of the amino acid residue in position 2 with a substituted alkyl chain gives rise to a more flexible backbone of the molecules with respect to analogues **1–3**. Moreover, when compounds **5** and **6** are compared, we can state that the dimethyl group located above the base of the L-shaped structure (analogue **6**) does not play a central role in increasing the sweet potency. An important role is played by the N-terminal 3-hydroxy-4-methyloxyphenyl group in increasing the sweet potency. Indeed, compounds **5** and **6** show the same potency but they are sweeter than compound **4**, where the N-terminal moiety is substituted by an terminal 3,3-dimethylbutyl group.

Conclusion

The results of the present investigation are consistent with our previous model which correlates the L-shaped structure with the sweet taste for aspartame-based peptide sweeteners. The preferred conformations found also fit the Tinti–Nofre model for sweet taste in which the N-substituted arylalkyl group occupies the D site of their model.

In conclusion, on the basis of this structure–activity study, we believe that the essential glucophores for a sweet compound arise from a suitable arrangement of the hydrophobic moiety (X) and the AH/B pairs, namely, the L-shaped conformation. However, other binding sites of the ligand can enhance sweet potency. In fact, the *N*-arylalkyl substitution enhances the sweetness potency of taste ligands, a fact suggesting the existence of an additional hydrophobic domain above the base of the L shape in the *x,y* plane.[9] From a comparison of the potency of unsubstituted aspartame-based taste ligands **8–10** with the *N*-arylalkyl-substituted molecules **1–3**, it is evident that the N-terminal chain above the base of the L shape (the D zone) might be responsible for the increase in the sweetness of these molecules. Our conformation studies have clearly indicated that the sweet taste of molecules in the L-shaped conformation can be amplified by an appropriately substituted residue 2 (the hydrophobic group X) arrayed over the base of the L shape. By comparing the potency and the structures of analogues **1–3**, we believe that the substitutions in the side chain of residue 2 play a fundamental role in enhancing the sweet potency because of the introduction of orientation constraints on the whole molecule. In particular, the incorporation of the $CH_2-S(CH_3)_3$ group as a side chain on residue 2 (analogue **1**) strongly enhances the sweetness potency of this taste ligand, whereas the 4-cyanophenyl group (analogue **3**) introduces more flexibility in to the structure as far as the relative orientation of the two hydrophobic groups in the molecule is concerned, probably due to a hydrophobic interac-

tion between the cyanophenyl moiety and the polar groups (the Asp NH_2^+ group and the side-chain Asp COO^- group).

On the other hand, analogues **4–6**, which bear the substituted alkyl chain 2-(S)-hydroxy-1-(R)-methyl-4-(S)-phenyl-hexyl-amide as the hydrophobic moiety X, show a more flexible backbone than the above-mentioned analogues (**1–3**). Moreover, our conformation study of compounds **4–6** (for compound **5** the crystal-state conformation was also determined by a single-crystal X-ray diffraction analysis) has shown that the 3-hydroxy-4-methyloxyphenyl *N*-arylalkyl terminal group (compounds **5** and **6**) increases the sweet potency with respect to the 3,3-dimethylbutyl *N*-alkyl group (analogue **4**) and also that the dimethyl group located above the base of the L-shaped structure (analogue **6**) does not play a central role. Indeed, the sweet potency of analogue **6** shows the same activity as that of analogue **5**. Finally, the analysis of the conformational features found by solution NMR spectroscopy and crystal-state X-ray diffraction analysis underlines the relevance of the $-x$ zone, as its occupancy by the OCH_3 group for analogues **1–3** and by the CH_3 group of position 6 of the hexylamide moiety for analogues **5** and **6** might be considered responsible (in addition to the L-shaped conformation) for the increase in their sweet taste.

Experimental Section

Peptide synthesis:

N-*[3-(3-Hydroxy-4-methoxyphenyl)-3-methylbutyl]-α-L-aspartyl-S-tert-butyl-L-cysteine 1-methylester (Compound 1)*: H-L-Cys(S*t*Bu)-OMe·HCl (2.03 g, 8.90 mmol; S*t*Bu = S-*tert*-butyl) was dissolved in dichloromethane (40 mL), and Boc-L-Asp(O*t*Bu)-OH.DCHA (4.19 g, 8.90 mmol; Boc = *tert*-butoxycarbonyl, O*t*Bu = O-*tert*-butyl, DCHA = dicyclohexylamine) was added. The solution was cooled to 0 °C, and EDC (1.88 g, 9.80 mmol; EDC = 1-ethyl-3-(3-dimethylaminopropyl)carbodiimide hydrochloricde) and HOBt (1.32 g, 9.80 mmol; HOBt = 1-hydroxybenzotriazole) were added. The mixture was stirred for 1 h at 0 °C and overnight at room temperature. The solvent was removed under reduced pressure, water (100 mL) was added, and the mixture was extracted twice with ethyl acetate (100 mL). The combined organic layers were washed twice with a 5% aqueous solution of citric acid (100 mL), with brine (50 mL), twice with a 5% aqueous solution of NaHCO₃ (100 mL), and finally with brine (50 mL). The solution was dried over MgSO₄, filtered, and concentrated under reduced pressure to obtain Boc-α-L-Asp(O*t*Bu)-L-Cys-(S*t*Bu)-OMe (4.10 g, 8.89 mmol) as a viscous oil. The protected dipeptide Boc-α-L-Asp(O*t*Bu)-L-Cys(S*t*Bu)-OMe (4.10 g, 8.89 mmol) was dissolved in HCl/dioxane (35 mL, 4 N) solution. The mixture was stirred for 2 h at room temperature and then concentrated under reduced pressure. The residue was suspended in water (50 mL) and the solution was neutralized with 30% aqueous solution of NH₃. The solvent was removed under reduced pressure and the residue was triturated with ethyl acetate (100 mL) and filtered. The filtrate was dried over MgSO₄, filtered, and concentrated under reduced pressure to obtain H-α-L-Asp-L-Cys(S*t*Bu)-OMe (2.20 g, 7.19 mmol) as a pale-yellow powder. The protected dipeptide H-α-L-Asp-L-Cys(S*t*Bu)-OMe (1.14 g, 3.72 mmol) was dissolved in THF (30 mL; THF = tetrahydrofuran) and the solution was cooled to 0 °C. Acetic acid (0.18 mL, 3.10 mmol), 3-methyl-3-(3-hydroxy-4-methoxyphenyl)butyraldehyde (0.65 g, 3.10 mmol), and NaB(OAc)₃H (0.99 g, 4.65 mmol; NaB(OAc)₃H = sodium triacetoxyborohydride)

were added. The mixture was stirred at 0 °C for 1 h and overnight at room temperature. Afterwards, saturated NaHCO₃ solution (30 mL) was added, and the solution was extracted twice with ethyl acetate (50 mL). The combined organic layers were washed with brine (50 mL) and dried over MgSO₄. After removal of MgSO₄ by filtration, the solution was concentrated under reduced pressure and the product was purified by preparative thin-layer chromatography on silica gel to obtain *N*-[3-(3-Hydroxy-4-methoxyphenyl)-3-methylbutyl]-α-ʟ-Asp-ʟ-Cys(StBu)-OMe (1.22 g, 2.45 mmol) as a solid: ^{1}H NMR ([D₆]dimethylsulfoxide (DMSO), 400 MHz): $\delta =$ 1.19 (s, 6H), 1.25 (s, 9H), 1.65–1.75 (m, 2H), 2.15–2.28 (m, 2H), 2.30–2.40 (m, 2H), 2.75–2.83 (m, 1H), 2.83–2.90 (m, 1H), 3.38–3.42 (m, 1H), 3.62 (s, 3H), 3.72 (s,3H), 4.40–4.45 (m, 1H), 6.67 (d, 1H), 6.75 (s, 1H), 6.79 (d, 1H), 8.56 ppm (d, 1H); ESI-MS: *m/z*: 499.38 [*M*+H]$^{+}$.

N-[3-(3-Hydroxy-4-methoxyphenyl)-3-methylbutyl]-α-ʟ-aspartyl-β-cyclohexyl-ʟ-alanine 1-methylester (Compound 2): H-ʟ-Cha-OMe·HCl (1.48 g, 6.49 mmol; Cha = β-cyclohexyl-ʟ-alanine) was dissolved in dichloromethane (30 mL), and Boc-ʟ-Asp(OBzl)-OH (2.10 g, 6.49 mmol; OBzl = *O*-benzyl) was added. The solution was cooled to 0 °C, and triethylamine (1.0 mL, 7.14 mmol), EDC (1.37 g, 7.14 mmol), and HOBt (0.97 g, 7.14 mmol) were added. The mixture was stirred 1 h at 0 °C and overnight at room temperature. The solvent was removed under reduced pressure, water (100 mL) was added, and the mixture was extracted twice with ethyl acetate (100 mL). The combined organic layers were washed twice with a 5 % aqueous solution of citric acid (100 mL), with brine (50 mL), twice with a 5 % aqueous solution of NaHCO₃ (100 mL), and finally with brine (50 mL). The solution was dried over MgSO₄, filtered, and concentrated under reduced pressure to obtain Boc-α-ʟ-Asp-(OBzl)-ʟ-Cha-OMe (3.16 g, 6.44 mmol) as a viscous oil. The protected dipeptide Boc-α-ʟ-Asp(OBzl)-ʟ-Cha-OMe (1.23 g, 2.50 mmol) was dissolved in 4 ɴ HCl/dioxane solution (12 mL). The mixture was stirred for 1 h at room temperature, concentrated under reduced pressure, and redissolved in 5 % aqueous solution of NaHCO₃ (100 mL). The solution was extracted twice with ethyl acetate (50 mL). The combined organic layers were washed with brine (50 mL) and dried over MgSO₄, filtered, and concentrated under reduced pressure to obtain H-α-ʟ-Asp(OBzl)-ʟ-Cha-OMe (0.96 g, 2.47 mmol) as a pale-yellow viscous oil. The protected dipeptide H-α-ʟ-Asp(OBzl)-ʟ-Cha-OMe (0.96 g, 2.47 mmol) was dissolved in THF (30 mL) and the solution was cooled to 0 °C. Acetic acid (0.14 mL, 2.47 mmol), 3-methyl-3-(3-hydroxy-4-methoxyphenyl)butyraldehyde (0.52 g, 2.47 mmol), and NaB(OAc)₃H (0.79 g, 3.71 mmol) were added. The mixture was stirred at 0 °C for 1 h and overnight at room temperature. Afterwards, saturated NaHCO₃ solution (30 mL) was added, and the solution was extracted twice with ethyl acetate (50 mL). The combined organic layers were washed with brine (50 mL) and dried over MgSO4. After removal of MgSO₄ by filtration, the solution was concentrated under reduced pressure and the product was purified by preparative thin-layer chromatography on silica gel to obtain *N*-[3-(3-hydroxy-4-methoxyphenyl)-3-methylbutyl]-α-ʟ-Asp(OBzl)-ʟ-Cha-OMe (0.98 g, 1.69 mmol) as a viscous oil. The protected dipeptide *N*-[3-(3-hydroxy-4-methoxyphenyl)-3-methylbutyl]-α-ʟ-Asp(OBzl)-ʟ-Cha-OMe (0.98 g, 1.69 mmol) was dissolved in a mixture of methanol (20 mL) and water (1 mL), and palladium on carbon (5 %, 0.45 g, water content = 50 %) was added. The mixture was placed under a hydrogen atmosphere for 4 h at room temperature. The catalyst was removed by filtration, the solvent was removed, and the product was dried under vacuum to obtain *N*-[3-(3-hydroxy-4-methoxyphenyl)-3-methylbutyl]- α-ʟ-Asp-ʟ-Cha-OMe (0.55 g, 1.07 mmol) as a solid: ^{1}H NMR ([D₆]DMSO, 400 MHz): $\delta =$ 0.75–0.98 (m, 2H), 1.05–1.30 (m, 3H), 1.18 (s, 6H), 1.50–1.75 (m, 10H), 2.10–2.25 (m, 2H), 2.30–2.40 (m, 2H), 3.41–3.45 (m, 1H), 3.60 (s, 3H), 3.72 (s, 3H), 4.30–4.38 (m, 1H), 6.67 (d, 1H), 6.75 (s, 1H), 6.79 (d, 1H), 8.43 ppm (d, 1H); ESI-MS: *m/z*: 493.54 [*M*+H]$^{+}$.

N-[3-(3-Hydroxy-4-methoxyphenyl)-3-methylbutyl]-α-ʟ-aspartyl-4-cyano-ʟ-phenylalanine 1-methylester (Compound 3): The compound was synthesized by using the procedure described for compound 2 with H-ʟ-Phe(4-CN)-OMe (4-cyano-ʟ-phenylalanine methyl ester) instead of H-ʟ-Cha-OMef·HCl to give *N*-[3-(3-hydroxy-4-methoxyphenyl)-3-methylbutyl]-α-ʟ-Asp-ʟ-Phe(4-CN)-OMe as a solid with an overall yield of 22.8 %: ^{1}H NMR ([D₆]DMSO, 400 MHz): $\delta =$ 1.12 (s, 6H), 1.55–1.70 (m, 2H), 2.00–2.18 (m, 3H), 2.22–2.30 (m, 1H), 2.93–3.00 (m, 1H), 3.10–3.20 (m, 1H), 3.28–3.32 (m, 1H), 3.60 (s, 3H), 3.71 (s, 3H), 4.50–4.60 (m, 1H), 6.63 (d, 1H), 6.73 (s, 1H), 6.81 (d, 1H), 7.39 (d, 2H), 7.72 (d, 2H), 8.50 ppm (d, 1H); ESI-MS: *m/z* = 512.31 [*M*+H]$^{+}$.

N-[3,3-Dimethylbutyl]-α-ʟ-aspartyl-(1R,2S,4S)-1-methyl-2-hydroxy-4-phenylhexylamide (Compound 4): (1*R*,2*S*,4*S*)-1-Methyl-2-hydroxy-4-phenylhexylamine (0.58 g, 2.80 mmol, 2*S*:2*R* > 5:1) was dissolved in dichloromethane (30 mL), and Boc-ʟ-Asp(OBzl)-OH (0.91 g, 2.80 mmol) was added. The solution was cooled to 0 °C, and EDC (0.59 g, 3.08 mmol) and HOBt (0.42 g, 3.08 mmol) were added. The mixture was stirred for 1 h at 0 °C and overnight at room temperature. The solvent was removed under reduced pressure, water (50 mL) was added, and the mixture was extracted twice with ethyl acetate (50 mL). The combined organic layers were washed twice with a 5 % aqueous solution of citric acid (50 mL), with brine (50 mL), twice with a 5 % aqueous solution of NaHCO₃ (100 mL), and finally with brine (50 mL). The solution was dried over MgSO₄, filtered, and concentrated under reduced pressure to obtain Boc-α-ʟ-Asp(OBzl)-(1*R*,2*S*,4*S*)-1-methyl-2-hydroxy-4-phenylhexylamide (1.43 g, 2.78 mmol) as a viscous oil. The amide Boc-α-ʟ-Asp(OBzl)-(1*R*,2*S*,4*S*)-1-methyl-2-hydroxy-4-phenylhexylamide (1.43 g, 2.78 mmol) was dissolved in 4 ɴ HCl/dioxane solution (7 mL). The mixture was stirred for 1 h at room temperature and then concentrated under reduced pressure and redissolved in 5 % aqueous solution of NaHCO₃ (50 mL). The solution was extracted twice with ethyl acetate (50 mL). The combined organic layers were washed with brine (50 mL), dried over MgSO₄, filtered, and concentrated under reduced pressure to obtain H-α-ʟ-Asp(OBzl)-(1*R*,2*S*,4*S*)-1-methyl-2-hydroxy-4-phenylhexylamide (1.13 g, 2.73 mmol) as a pale-yellow viscous oil. The amide H-α-ʟ-Asp(OBzl)-(1*R*,2*S*,4*S*)-1-methyl-2-hydroxy-4-phenylhexylamide (1.13 g, 2.73 mmol) was dissolved in THF (20 mL) and the solution was cooled to 0 °C. Acetic acid (0.16 mL, 2.73 mmol), 3,3-dimethylbutyraldehyde (0.34 mL, 2.73 mmol), and NaB(OAc)₃H (0.87 g, 4.10 mmol) were added. The mixture was stirred at 0 °C for 1 h and overnight at room temperature. Afterwards, saturated NaHCO3 solution (30 mL) was added, and the solution was extracted twice with ethyl acetate (50 mL). The combined organic layers were washed with brine (50 mL) and dried over MgSO₄. After removal of MgSO₄ by filtration, the solution was concentrated under reduced pressure and the product was purified by preparative thin-layer chromatography on silica gel to obtain *N*-(3,3-dimethylbutyl)-α-ʟ-Asp(OBzl)-(1*R*,2*S*,4*S*)-1-methyl-2-hydroxy-4-phenylhexylamide (1.04 g, 2.09 mmol) as a pale-yellow viscous oil. The amide *N*-(3,3-dimethylbutyl)-α-ʟ-Asp(OBzl)-(1*R*,2*S*,4*S*)-1-methyl-2-hydroxy-4-phenylhexylamide (2.09 mmol, 1.04 g) was dissolved in a mixture of methanol (40 mL) and water (5 mL), and palladium on carbon (5 %, 0.50 g, water content = 50 %) was added. The mixture was placed under a hydrogen atmosphere overnight at room temperature. The catalyst was removed by filtration, the solvent was removed, and the product was dried under

vacuum to obtain *N*-(3,3-dimethylbutyl)-α-L-Asp-(1*R*,2*S*,4*S*)-1-methyl-2-hydroxy-4-phenylhexylamide (1.81 mmol, 0.74 g) as a solid: ^{1}H NMR ([D$_6$]DMSO, 400 MHz): $\delta = 0.66$ (t, 3H), 0.83 (s, 9H), 1.00 (d, 3H) 1.35–1.56 (m, 4H), 1.63–1.76 (m, 2H), 2.55–2.72 (m, 5H), 3.40–3.48 (m, 1H), 3.75–3.88 (m, 2H), 4.70 (br s, 1H), 7.10–7.30 (m, 5H), 8.34 ppm (d, 1H); ESI-MS: *m/z*: 407.40 [*M*+H]$^+$.

N-[3-(3-Hydroxy-4-methoxyphenyl)propyl]-α-L-aspartyl-(1*R*,2*S*,4*S*)-1-methyl-2-hydroxy-4-phenylhexylamide (Compound 5): The compound was synthesized by using the procedure described for compound **4** with 3-benzyloxy-4-methoxycinnamaldehyde instead of 3,3-dimethylbutyraldehyde to give *N*-[3-(3-hydroxy-4-methoxyphenyl)propyl]-α-L-aspartyl (1*R*,2*S*,4*S*)-1-methyl-2-hydroxy-4-phenylhexylamide as a solid with an overall yield of 33.5%: ^{1}H NMR ([D$_6$]DMSO, 400 MHz): $\delta = 0.64$–0.67 (m, 3H), 0.98–1.00 (m, 3H), 1.42–1.48 (m, 2H), 1.63–1.69 (m, 4H), 2.22–2.40 (m, 2H), 2.41–2.44 (m, 2H), 2.58–2.61 (m, 1H), 3.35–3.40 (m, 4H), 3.71 (s, 3H), 3.73 (m, 1H), 4.57–4.71 (br s, 1H), 6.53–6.61 (m, 2H), 6.77–6.80 (m, 1H), 7.13–7.15 (m, 3H), 7.26–7.28 (m, 2H), 7.93–7.95 (m, 1H), 8.68–8.92 ppm (br s, 1H); ESI-MS: *m/z*: 487.47 [*M*+H]$^+$.

N-[3-(3-Hydroxy-4-methoxyphenyl)-3-methylbutyl]-L-α-aspartyl-(1*R*,2*S*,4*S*)-1-methyl-2-hydroxy-4-phenylhexylamide (Compound 6): The compound was synthesized by using the procedure described for compound **4** with 3-methyl-3-(3-benzyloxy-4-methoxyphenyl) butyraldehyde instead of 3,3-dimethylbutyraldehyde to give *N*-[3-(3-hydroxy-4-methoxyphenyl)-3-methylbutyl]-L-α-aspartyl-(1*R*,2*S*,4*S*)-1-methyl-2-hydroxy-4-phenylhexylamide as a solid with an overall yield of 53.0%: ^{1}H NMR ([D$_6$]DMSO, 400 MHz): $\delta = 0.64$–0.68 (m, 3H), 0.95–0.97 (m, 3H), 1.16 (s, 6H), 1.41–1.48 (m, 2H), 1.64–1.80 (m, 4H), 2.08–2.34 (m, 4H), 2.58–2.62 (m, 1H), 3.30–3.37 (m, 2H), 3.71 (s, 3H), 4.58–4.64 (br s, 1H), 6.63–6.65 (m, 1H), 6.75–6.79 (m, 2H), 7.14–7.18 (m, 3H), 7.25–7.28 (m, 2H), 7.86–7.88 (m, 1H), 8.68–8.81 ppm (br s, 1H); ESI-MS: *m/z*: 515.51 [*M*+H]$^+$.

^{1}H NMR spectra were measured by using a Bruker AVANCE 400 (400 MHz) instrument for solutions in [D$_6$]DMSO with tetramethylsilane as the internal reference. Mass spectra were taken with a Thermo Quest TSQ 700 instrument. Merck precoated silica gel 60 F$_{254}$ plates of 0.25 or 1.0 mm thickness were used for analytical or preparative thin-layer chromatography, respectively. The amino acid derivatives, *N*-tert-butoxycarbonyl-*S*-tert-butyl-L-cysteine dicyclohexylammonium salt, β-cyclohexyl-L-alanine hydrochloride, and 4-cyano-L-phenylalanine were purchased from Bachem, Switzerland, and were transformed into their methyl ester derivatives by conventional methods. 3,3-Dimethylbutyraldehyde was purchased from Sigma–Aldrich Co. (1*R*,2*S*,4*S*)-1-methyl-2-hydroxy-4-phenylhexylamine was synthesized by a previously reported method.[9] Taste tests were carried out by a "sip and spit" taste assessment of solutions of the molecules by members of our research group. All the compounds were tested in water at room temperature without any pH adjustment. The taste solutions were diluted as necessary in order to match a 4% sucrose solution used as our standard. The ratio of a 4% sucrose solution perceived as equally sweet to the actual concentration of the test compound is the sweetness potency quoted in this report.

X-ray diffraction analysis: Colorless single crystals of compound **5** were grown at room temperature by slow evaporation of a methanol/water mixture. X-ray diffraction data were collected on an Enraf–Nonius CAD4 diffractometer (Delft, The Netherlands) at the Institute of Biostructures and Bioimaging of C.N.R. at the University of Naples "Federico II". The sweetener compound crystallizes in the monoclinic system, space group *P*2$_1$. The intensities were corrected for Lorentz and polarization factors, but no absorption correction

was applied. The structure was solved by direct methods by using the SIR97 program.[12] The solution with the best figure of merit revealed the coordinates of all non-hydrogen atoms of the compound. The structure was refined by using the SHELXL-97 program[13] by a full-matrix least-square procedure on F^2 (all data) with anisotropic thermal factors for all non-hydrogen atoms. Difference Fourier analysis revealed the two hydrogen atoms of the water molecule. The hydrogen-atom positions of the sweetener compound were calculated. During the refinement all hydrogen atoms were allowed to ride on their carrying atoms, with the U_{iso} value set equal to 1.2 times the U_{eq} value of the attached atom.

The scattering factors for all atomic species were calculated from Cromer and Waber.[14] Details of the crystallographic data and diffraction parameters are given in Table 5. CCDC-280299 contains the supplementary crystallographic data for this paper. These data can be obtained free of charge from The Cambridge Crystallographic Data Centre via www.ccdc.cam.ac.uk/data_request/cif.

Table 5. Crystal data for *N*-[3-(3-hydroxy-4-methoxyphenyl)propyl]-α-L-aspartyl-(1*R*,2*S*,4*S*)-1-methyl-2-hydroxy-4-phenylhexylamide (**5**).

empirical formula	$C_{27}H_{38}N_2O_6$
formula weight	486.59
wavelength [Å]	1.54178
crystal system	monoclinic
space group	$P2_1$
unit cell dimensions [Å / °]	$a = 12.846$ (3)
	$b = 7.388$ (3), $\beta = 91.86(1)$
	$c = 14.370$ (4)
V [Å^3]	1363.1(7)
Z	2
ρ_{calcd} [mg m^{-3}]	1.186
absorption coefficient [mm^{-1}]	0.678
$F(000)$	524
θ range for data collection [°]	3.08–70.04
independent reflections	2763
reflections with [$I > 2\sigma(I)$]	2265
refinement method	full-matrix least-squares on F^2
data/restraints/parameters	2763/1/317
goodness-of-fit on F^2	1.436
final *R* indices [$I > 2\sigma(I)$]	$R1 = 0.0624$, $wR2 = 0.1763$
R indices (all data)	$R1 = 0.0723$, $wR2 = 0.1820$
largest diff. peak and hole [e Å^{-3}]	0.220 and −0.229

^{1}H NMR measurements: The ^{1}H NMR spectra were recorded on a Bruker AMX500 spectrometer operating at 500 MHz. All experiments were carried out in fully deuterated DMSO with the solvent peak as an internal standard. The concentration of samples was around 5 mM. All 2D NMR spectra were recorded in phase-sensitive mode by using time-proportional phase-increment (TPPI) and quadrature detection in both dimensions. The peak assignments were made by using TOCSY[15,16] and ROESY[17,18] experiments. The TOCSY experiments were performed by using the MELV-17 spinlock sequence with a spin-locking field of 10 kHz and mixing times of 50 and 70 ms. The ROESY experiments were carried out by using mixing times of 50, 100, and 200 ms with a spin-locking field of 2.5 kHz. The TOCSY and ROESY results were obtained by using 2000 data points in the f_2 domain and 256 points in the f_1 domain. Zero filling was applied in the f_1 and f_2 domains to obtain a matrix of 2000 × 2000 data points. DQF-COSY data were acquired by using 4000 data points in the f_2 domain in order to have a higher digital resolution. Multiplication with a phase-shifted sinebell function was employed to enhance the spectra. Chemical shifts were referenced to [D$_6$]DMSO (2.49 ppm). The $J_{HN-H\alpha}$ and $J_{H\alpha\beta}$ coupling

constants were obtained from 1D spectra and by sections of cross-peaks from the resolution-enhanced 4000 × 2000 DQF-COSY spectra. NOE cross-peak volumes were calibrated against the distance between the two β protons of the Asp residue on the basis of ISPA (isolated spin-pair approximation).[19] On the basis of a comparison with other known distances, an error of approximately ±0.5 Å was estimated. Consequently, the upper and lower distance constraints were set to the measured distances ± 0.5 Å, respectively. The restraints were classified as strong, medium, and weak with distance upper limits of 2.5, 3.5, and 4.5 Å, respectively. The ϕ angles were calculated by using a Karplus-type relationship reported by Bystrov et al.[20a] and Cung and Marraud.[20b] The stereospecific assignment of the β protons, required for the calculation of the side-chain population, was achieved by following the procedure reported by Yamazaki et al.[11] The side-chain population was calculated by using the Pachler's values[21] $J_T = 13.56$ and $J_G = 2.60$ for aliphatic residues and the Cung's values[22] $J_T = 13.85$ and $J_G = 3.55$ for aromatic residues, respectively.

Computer simulations: The computational protocol for structural determination in solution consisted of distance geometry (DG) conformation search, energy-minimization, and molecular dynamics (MD) simulations. The distance geometry module of the Insight II program,[23] was used to generate 100 structures consistent with the distance restraints derived from the NOE intensities. The structures, after distance geometry, were subjected to restrained minimization by employing the DISCOVER module of the Insight II program,[23] with a CVFF91 force field and the VA09A algorithm with a convergence criterion of 0.01 kcal mol^{-1} Å^{-1}. All calculations were carried out in vacuo and a distance-dependent dielectric constant was used to take into account the solvent effects.[24] In the simulations, the peptide bonds were maintained in the *trans* conformation.

The torsion angles and the NOE distances of these structures were compared with the values derived from NMR measurements. A Karplus-type equation[25] was used to compute the torsion values consistent with the measured $J_{HN-H\alpha}$ coupling constants, and an error of ±30° was tolerated. Structures not consistent with the experimentally derived torsional angles and distance restraints were discarded. A cutoff of 5 kcal mol^{-1}[26] above the average-energy conformer was used to sort out unrealistically high-energy conformations of the remaining structures. A cluster analysis[27] was performed by first extracting the mean-energy conformer out of all the conformations under investigation. Prior to every molecular dynamics simulation, the system was equilibrated with 50 ps of initialization dynamics. In an attempt to carry out a thorough search of the accessible conformational space, each average-energy conformation of the clusters was subjected to 600 ps of restrained molecular dynamics at 500 K with a step size of 1 fs. The conformers that were consistent with the experimental data were subjected to the same cluster analysis as described above. Finally, the mean-energy structure of each cluster was chosen as the preferred conformation in solution for the sweetener analogues.

Unrestrained molecular dynamics simulations at 300 K with a distance-dependent dielectric constant of 1 were carried out. The selected conformers were first submitted to 50 ps of equilibrium, followed by a step size of 1 fs for a 1 ns simulation. Structures were collected every 10 ps to obtain the predominant molecular conformations in solution. For our studies we assume that the "bioactive" conformation of a taste ligand would be one of the accessible mean conformations of the isolated ligand in solution. We contend that interactions of receptors with ligands cannot convert inaccessible high-energy structures to allowed conformations.

[1] D. E. Walters, I. Prakash, N. Desai, *J. Med. Chem.* **2000**, *43*, 1242–1245.

[2] a) G. Morini, A. Bassoli, P. A. Temussi, *J. Med. Chem.* **2005**, *48*, 5520–5529; b) H. Xu, L. Staszewski, H. Tang, E. Adler, M. Zoller, X. Li, *Proc. Natl. Acad. Sci. USA* **2004**, *101*, 14258–14263.

[3] T. Yamazaki, E. Benedetti, D. Kent, M. Goodman, *Angew. Chem.* **1994**, *106*, 1502–1517; *Angew. Chem. Int. Ed. Engl.* **1994**, *33*, 1437–1451.

[4] a) L. B. Kier, *J. Pharm. Sci.* **1972**, *61*, 1394–1395; b) R. S. Shallenberger, M. G. Lindley, *Food Chem.* **1977**, *2*, 145–153.

[5] J. M. Tinti, C. Nofre in *Sweeteners: Discovery, Molecular Design, and Chemoreception* (Eds.: D. E. Walters, F. T. Orthoefer, G. Dubois), American Chemical Society, Washington, DC, **1991**, pp. 206–213.

[6] M. Goodman, J. R. Del Valle, Y. Amino, E. Benedetti, *Pure Appl. Chem.* **2002**, *74*, 1109–1116.

[7] L. B. P. Brussel, H. G. Peer, A. Z. van der Heijden, *Z. Lebensm.-Unters. Forsch.* **1975**, 159, 337–343.

[8] R. H. Mazur, J. A. Reuter, K. A. Swiatek, J. M. Schlatter, *J. Med. Chem.* **1973**, *16*, 1284–1287.

[9] R. H. Mattern, Y. Amino, E. Benedetti, M. Goodman, *J. Pept. Res.* **1997**, *50*, 286–299.

[10] M. Goodman, S. Yang, unpublished results.

[11] T. Yamazaki, A. Probsti, P. W. Schiller, M. Goodman, *Int. J. Pept. Protein Res.* **1991**, *37*, 364–381.

[12] A. Altomare, M. C. Burla, M. Camalli, G. Cascarano, C. Giacovazzo, A. Guagliardi, A. G. G. Moliterni, G. Polidori, R. Spagna, SIR97: A Program for Automatic Solution and Refinement of Crystal Structures, University of Bari, Italy, **1997**.

[13] G. M. Sheldrick, SHELXL97: Program for Crystal Structure Refinement, University of Göttingen, Germany, **1997**.

[14] D. T. Cromer, J. T. Waber, *International Tables for X-Ray Crystallography*, Vol. IV, Kynoch, Birmingham, UK, **1974**, Table 2.2B.

[15] a) W. P. Aue, E. Bartholdi, R. R. Ernst, *J. Chem. Phys.* **1976**, *64*, 2229–2246; b) G. Bodenhausen, *J. Magn. Reson.* **1980**, *B37*, 93–106; c) A. Bax, R. Freeman, *J. Magn. Reson.* **1981**, *44*, 542–561.

[16] a) M. Rance, O. W. Sørensen, G. Bodenhausen, G. Wagner, R. R. Ernst, K. Wüthrich, *Biochem. Biophys. Res. Commun.* **1983**, *117*, 479–485; b) D. Davis, A. Bax, *J. Am. Chem. Soc.* **1985**, *107*, 2820–2821.

[17] A. A. Bothner-By, R. L. Stephens, J. Lee, C. D. Warren, R. W. Jeanloz, *J. Am. Chem. Soc.* **1984**, *106*, 811–813.

[18] K. Wüthrich, *NMR of Proteins and Nucleic Acids*, Wiley, New York, **1986**.

[19] P. D. Thomas, V. J. Basus, T. L. James, *Proc. Natl. Acad. Sci. USA* **1991**, *88*, 1237–1241.

[20] a) V. F. Bystrov, V. T. Ivanov, S. L. Portanova, T. A. Balashova, Y. A. Ovchinnikov, *Tetrahedron* **1973**, *29*, 873–877; b) M. T. Cung, M. Marraud, J. Neél, *Macromolecules* **1974**, *7*, 606–613.

[21] K. G. P. Pachler, *Spectrochim. Acta* **1964**, *20*, 581–587.

[22] M. T. Cung, M. Marraud, *Biopolymers* **1982**, *21*, 953–967.

[23] InsightII and Discover User Guides (Versions 2000 and 2.98), Molecular Simulation 2000, San Diego, **2000**.

[24] A. R. Leach, *Molecular Modeling, Principles and Applications*, Addison Wesley Longman, Essex, **1996**.

[25] M. Karplus, *J. Am. Chem. Soc.* **1963**, *85*, 2870–2871.

[26] W. M. Kazmierski, R. D. Ferguson, A. W. Lipkowski, V. J. Hruby, *Int. J. Pept. Protein Res.* **1995**, *46*, 256–278.

[27] T. Yamazaki, D. F. Mierke, O. E. Said-Nejad, E. R. Felder, M. Goodman, *Int. J. Pept. Protein Res.* **1992**, *39*, 161–181.